Reactions Involving the Nuclear Spin Modifications of H_3^+ and H_2; Implications for the Interstellar Medium

Brian A. Tom

Preliminary Examination

Department of Chemistry

University of Illinois at Urbana-Champaign

29 August 2008

I. INTRODUCTION

Hydrogen is the most abundant element in the universe, comprising 92.1% by total number. Due to this abundance, chemical processes in the interstellar medium are largely governed by hydrogenic species [1]. The H_2 in these regions of space is ionized by cosmic rays at a rate of 4×10^{-16} s^{-1} [2]. The dominant ionic species in the resultant plasma is H_3^+ [3], with the reaction $H_2^+ + H_2 \rightarrow H_3^+ + H$ ($k_L = 2 \times 10^{-9}\,cm^3\,s^{-1}$) serving as the primary formation pathway. Subsequently, H_3^+ reacts to form many heavier polyatomics [4, 5].

The existence of two forms of H_2, differing by the relative alignment between proton intrinsic spins, was first predicted in 1927 [6, 7], and experimentally observed shortly thereafter [8]. The symmetrically-aligned *ortho*-H_2 spin modification (I=1) and the anti-aligned *para*-H_2 (I=0) exist with a spin degeneracy ratio of 3:1. H_3^+ also exists in two forms, *ortho* (I=3/2) and *para* (I=1/2).

Observations of the hydrogenic column densities along various sightlines, as well as the distribution between the *ortho* and *para* spin modifications, have been useful tools in determining cloud dimensions, temperatures [9], cloud densities [1], and the aforementioned cosmic-ray ionization rate [2]. Nevertheless, problems have arisen regarding the distributions between the two spin modifications in the interstellar medium. Temperature has been inferred in diffuse interstellar clouds using both the ratio of *ortho*- to *para*-H_2, and the ratio of *ortho*- to *para*-H_3^+. Surprisingly, the temperature inferred with H_2 is 30-40 K higher than from the H_3^+, which indicates a gap in our understanding of how H_3^+ is partitioned between the *ortho* and *para* states. The *ortho*:*para* distribution of molecular hydrogen in dense clouds also presents an interesting astrochemical problem. The *para*-H_2 fraction is enriched to a level consistent with thermalization at the temperatures of these clouds [10, 11], but the process by which this occurs is not well understood.

Two likely candidates for the diffuse cloud disparity are the state-specific destruction of H_3^+ by dissociative recombination, and the reaction $H_3^+ + H_2 \rightarrow H_2 + H_3^+$, which is capable of changing the spin state of both the ion and H_2. The latter process could also be responsible for the dense cloud *para*-H_2 fraction. My research is focused on understanding these processes, not only to answer the astrophysical questions, but also to shed light on these very interesting and fundamental reactions involving the simplest of all molecules.

II. PROGRESS

A. Destruction of *para*-H_3^+: Dissociative Recombination with Electrons

Dissociative recombination (DR) is the primary destructive pathway for H_3^+ in diffuse interstellar clouds. In this process, an H_3^+ ion captures an electron and dissociates into either H_2 + H, or 3H. In 2002, the DR rate of rotationally cold H_3^+ was measured at the CRYRING ion storage ring in Stockholm [12], and subsequently verified at the Test Storage Ring (TSR) in Heidelberg [13]. These measurements were acquired using a normal H_2 (*ortho*:*para*=3:1) feed gas. According to early theoretical predictions [14], there should be a difference between the recombination cross sections of the two spin modifications of H_3^+, with the *ortho* states possessing a higher recombination rate. An initial attempt to measure this at TSR with a greater, but not precisely known, *para*-H_3^+ enrichment demonstrated that a difference existed, but in the opposite sense [13]. Revisions to theory suggested that the *para*-H_3^+ spin modification should indeed possess a higher recombination rate [15].

Our objective was to observe the DR of *para*-H_3^+ ions at an astrophysically relevant temperature, and in so doing measure for the first time the recombination rate of a single quantum state. To do this we designed and built a *para*-H_2 converter using a closed-cycle ^{4}He cryostat [16]. This converter is capable of generating $> 99.9\%$-enriched *para*-H_2, which we measure using a modified thermal conductance cell [17, 18], as well as a nuclear magnetic resonance technique. We stored the *para*-H_2 gas in a teflon-lined sample bottle to minimize back conversion.

For the experiment, the ion source consisted of a solenoid valve with a 500 μm pinhole through which the test gas was pulsed at a frequency of 0.1 Hz. Ionization occurred when the test gas expanded through a ring-electrode held at -350 to -500 volts. The collisions in the Campargue-type expansion resulted in translational and rotational cooling of the ions [19] to temperatures comparable to those found in the interstellar medium. It was possible to generate a plasma highly enriched in *para*-H_3^+ because, according to spin selection rules, only *para*-H_3^+ can form when using a pure *para*-H_2 feed gas [20, 21].

In order to verify that the plasma generated by the source was both cold and highly enriched in *para*-H_3^+, it was necessary to perform a spectroscopic characterization both before and after the experimental runs at CRYRING. The structure of H_3^+ is an equilateral triangle

with D_{3h} symmetry. It possesses no permanent electric dipole moment and therefore no allowed pure rotational spectrum, nor are there stable excited electronic states available for optical spectroscopy [22]. Consequently, the only tool available to observational astronomer and experimental spectroscopist alike is the mid-infrared rovibrational spectrum.

We used a Difference Frequency Generation (DFG) laser to perform cavity ringdown spectroscopy in our analysis [23]. The DFG was pumped with a cw-Nd:YAG laser which was mixed with a tunable cw-Ti:Sapphire ring laser in a heated periodically-poled $LiNbO_3$ crystal. The resultant 3.67 μm beam was coupled into a $\sim$0.75 m high finesse cavity formed by two 99.98% reflective mirrors, one of which was dithered in order to bring the cavity in and out of resonance with the DFG mid-IR idler output. In order to perform ringdown spectroscopy with the pulsed source we developed a routine in LabWindows which predicted the ringdown events, and activated the source so that ions were present when ringdown occurred.

We observed the $\nu_2 \leftarrow 0$ transitions from the ground states of *ortho-* and *para*-H_3^+, (1,0) and (1,1) respectively, where the labeling represents (J,K) [24]. These are depicted in Figure 1 (all figures and tables are presented at the end of this document). For both the temperature and enrichment measurements, we compared the relative absorptions of $R(1,0)$ and $R(1,1)^u$ as a proxy for the relative ion populations. The temperature we measured from these peaks was an "excitation" temperature based on the distribution of *ortho* and *para* states, and we found it to correlate well with the true rotational temperature measured using a transition from the next rotationally excited state of *para*-H_3^+, (2,2). The temperature of our expansion was between 70-100K, close to the average temperature of diffuse interstellar clouds [2].

We applied corrections to subsequent $R(1,0)$ and $R(1,1)^u$ peak measurements using a Maxwell-Boltzmann distribution for 70-100 K. This was done in order to more accurately compare the total *ortho*-H_3^+ with the total *para*-H_3^+ for the enrichment measurements. With the objective of maximizing the *para*-H_3^+ fraction of the plasma, we diluted the H_2 feed gas in argon. This helped reduce the number of $H_3^+ + H_2$ collisions, thereby reducing conversion of *para*-H_3^+ to *ortho*-H_3^+ (see next section). The results of the enrichment experiments are depicted graphically in Figure 2, and in Table I.

At the CRYRING ion storage ring, the pulsed source injected translationally and rotationally cold ions which were then accelerated to 12.1 MeV and stored for approximately

10 seconds before measurement. The storage time allowed the ions to vibrationally relax before recombining with monoenergetic electrons in an electron cooler [25]. Recombination events were counted when the neutral fragments, no longer subject to the electromagnetic forces of the ring bending magnets, exited the ring and hit a surface barrier detector.

The results of the experiment are presented in Figure 3 [26]. We observed an increase in the DR rate over normal H_2 with both the undiluted *para*-H_2 sample as well as the 1% dilution. These recombination spectra represent the rates for 50, 74, and 83%-enriched *para*-H_3^+ plasmas based on a 97% *para*-enriched H_2 feed gas. Unfortunately, our source did not produce ions as rotationally cold as it had in the past [12], and the ions also appeared to have undergone rotational heating during storage. Consequently, we could only make a relative comparison between results taken with different *para*-H_3^+ enrichments. Nevertheless, we were able to use these measurements to extrapolate relative rate coefficient spectra for 100% *ortho*- and *para*-H_3^+ plasmas, also shown in Figure 3. The results indicate there is a 2-fold difference between the rates of recombination for pure *ortho*- and *para*-H_3^+ at low electron energies. From this initial measurement, DR does not appear to play the dominant role in the partitioning of H_3^+ spin modifications in diffuse clouds, and the increase in the rate coefficient for interstellar *para*-H_3^+ certainly cannot explain the *enrichment* of the *para*-H_3^+ fraction.

B. Spin State Conversion in the Reaction $\mathbf{H_3^+ + H_2 \rightarrow H_2 + H_3^+}$

The reaction of H_3^+ with H_2 is another pathway that could lead to the enigmatic enrichment of the *para*-H_3^+ fraction in diffuse clouds (the *para*-H_2 fraction in dense clouds is addressed later). Evidence of this can be seen in Table I where the 99.9% *para*-H_2 feed gas only produces a 77.6% *para*-H_3^+ enriched plasma. According to the spin selection rules for $H_2^+ + H_2$, this enrichment should be much closer to 99.9%, and our observed difference can only be due to the transfer of protons between the ion and molecular hydrogen. The reaction of H_3^+ with H_2 can proceed in one of three ways: *identity* in which no proton transfer takes place (1), *hop* in which it appears that a single proton transfers from the H_3^+ to the H_2 (2), and *exchange* where a single proton moves from the H_2 to the H_3^+, and vice versa (3).

$$H_3^+ + \tilde{H}_2 \rightarrow H_3^+ + \tilde{H}_2, \tag{1}$$

$$H_3^+ + \tilde{H}_2 \rightarrow H\tilde{H}_2^+ + H_2, \quad (2)$$

$$H_3^+ + \tilde{H}_2 \rightarrow H_2\tilde{H}^+ + H\tilde{H}, \quad (3)$$

Using angular momentum algebra and the initial enrichment of *para*-H_2, it is possible to derive the distribution of spin modifications amongst the product H_3^+ states of the $H_2^+ + H_2$ reaction. In similar fashion, one can derive the distribution of *ortho* and *para*-H_3^+ and H_2 states resulting from reactions (1 - 3), and these values are shown in Table II. An inspection of the rows in which the reactants include *para*-H_3^+ shows that the product *ortho*-H_3^+:*para*-H_3^+ ratio is strongly dependent on which type of reaction takes place, *hop* or *exchange*. Thus it is important to understand the ratio $\alpha = k_{Hop}/k_{Exchange}$, and in particular how it is affected by temperature. The temperature dependence of α was observed in experiments with deuterated species [27], and the ratio was measured with hydrogen in a hollow cathode experiment [28] to be $\alpha = 2.4$ at $T_{rot} = 400$-450 K.

In order to observe α at colder temperatures, we performed measurements using the same experimental setup described in the DR section. The data we collected were the inferred fraction of *para*-H_3^+ in our expansion for a given *para*-H_2 feed gas enrichment. The *para*-H_3^+ fraction was measured using 5 different *para*-H_2 enrichments (see Table III).

Assuming steady state for the *para*-H_3^+ fraction, we derived an analytic solution that related the fraction of *para*-H_3^+ in the plasma with the fraction of *para*-H_2 in the feed gas using the detailed rate equations [28]. The simple result is,

$$f_p = (\alpha + 2\alpha\gamma + 1)/(3\alpha + 2) \quad (4)$$

where f_p is the fraction of *para*-H_3^+ in the expansion, and γ is the fraction of *para*-H_2.

The results are presented in Table III, and graphically in Figure 4. We determined that $\alpha \sim 0.78$ in the temperature range $T_{rot} = 70$-100 K, indicating that the exchange reaction is dominant at lower temperatures. The $\alpha \sim 0.78$ result provides a tentative explanation of the diffuse cloud observations in which there is an enrichment of *para*-H_3^+. Combining our value of $\alpha \sim 0.78$ and a representative $\gamma = 0.52$ for diffuse clouds [29] in Equation (4), we predict a *para*-H_3^+ fraction of $f_p = 0.60$. This is in good agreement with the observed value $f_p = 0.65$ which is the average from 9 diffuse cloud sight lines (N. Indriolo, private communication).

III. FUTURE WORK

A. Dissociative Recombination

In order to make a definitive measurement of the DR rate for *para*-H_3^+ enriched in a single quantum state, we intend to perform another experiment at CRYRING. The spectra depicted in Figure 3 are not in a form that is useful for astrophysical application. Instead, each spectrum must be integrated with a Maxwell-Boltzmann distribution of electron energies at a given temperature in order to calculate a thermal rate coefficient. As mentioned earlier, we could not confidently calculate an accurate thermal rate coefficient for a single state of *para*-H_3^+ because of the uncertainty in our T_{rot}.

Our next experiment will involve the same steps described earlier, with some significant improvements. First we intend to re-design the source around a piezo instead of a solenoid valve. The T_{rot} of the expansion from the solenoid design was highly susceptible to valve tuning and poppet condition, and as such was somewhat unstable. Although the piezo design will initially require tuning, it should be capable of consistently producing rotationally cold ions once tuned [30].

There are plans for our collaborators in Stockholm to bake the electron cooler section of the ring prior to the next run. Baking is long-overdue maintenance, and will reduce the number of residual collisions that could lead to rotational heating of the ions in the ring. We also plan to perform a thorough ion current calibration to eliminate a vertical offset that we observed in our spectra. This should obviate the need to normalize our data to past experiments, a procedure that was required with our most recent results.

With the new measurements we will be able to calculate absolute thermal rate coefficients useful for diffuse interstellar models. We will also be able to predict the recombination rates for 100% *ortho*- and 100% *para*-H_3^+, this time at temperatures we know to be astrophysically relevant.

B. Continuing α Measurements

Although our value of α seems to explain astronomical observations, the theory we applied to our data does not, in principle, accurately reflect what is physically happening in the $H_3^+ + H_2$ reaction. The product distributions depicted in Table II are only valid for

interactions that occur at high temperatures ($\sim$ 200 K and warmer). This is because at colder temperatures, any reaction where *para*-$H_2 \rightarrow$ *ortho*-H_2 is unlikely to proceed due to the 120 cm^{-1} energy difference that exists between the *ortho*- and *para*-H_2 ground states. In addition, the high temperature model incorrectly treats all excited states of H_3^+ as being equally available, no matter what the energy.

Park and Light [31] developed a new theory for colder temperatures that accounts for the errors of the high temperature model. They calculated the rate coefficients for the same reactant and product combinations as depicted in Table II, however, they did so with the aid of a so called cumulative reaction probability (CRP). The CRP is a product of the probabilities for complex formation, proton scrambling, and spin modification. The results from the low temperature model vary significantly with temperature, but the predicted branching ratios converge on the values of Table II at the high temperature limit. In Figure 4, we have shown the behavior of α as predicted by this low temperature model alongside the behavior predicted with the high temperature model. Although our data were taken in the low temperature regime, the distribution of *para*-H_2 enrichments (γ) was such that we could not determine if the points track linearly with the high temperature predictions, or non-linearly with the low temperature α predictions. The data at the point where $\gamma = 25\%$ indicates some degree of error in the low temperature model.

Ultimately, the temperature dependence of α could be due to a real change in $k_{\mathrm{Hop}}/k_{\mathrm{Exchange}}$ as predicted by the high temperature model, or it could be an apparent change in this ratio due to the energy and availability of states, as predicted by low temperature theory. We can take the first steps towards understanding this by examining the behavior of the *para*-H_3^+ fraction (f_p) over a wider range of *para*-H_2 fractions (γ) in the feed gas.

1. Hollow Cathode

We have built a hollow cathode with which to explore the $H_3^+ + H_2$ reaction at different temperatures [32]. With water cooling we can generate plasmas with $T_{rot} > 400$ K, and with liquid nitrogen we can achieve $T_{rot} = 120 \pm 10$ K [33]. The hollow cathode experiments will employ a multipass White-cell configuration [34] to perform direct absorption spectroscopy. This will allow us to measure the time-dependent behavior of the *ortho*- and *para*-H_3^+.

The first experiment will be run at T_{rot} = 400-450 K. In this temperature regime, we

can verify our new experimental setup by comparing our results with those of [28]. The $R(1,0)$ and $R(1,1)^u$ transitions will be monitored during a series of discharge pulses that last up to ten milliseconds. These measurements will give us the time-dependent *para*-H_3^+ fraction (f_p), which in conjunction with the *para*-H_2 fraction (γ) can be used in equation (4) to calculate α. The ability to measure γ will be discussed in the next section. We expect the relationship between f_p and γ to be linear at high temperature.

The next set of measurements will be taken using liquid nitrogen as the coolant. These experiments will measure f_p and γ at a temperature intermediate to our previous results ($T_{rot} \sim 120$ K). According to the low temperature theory [31], we expect to see a nonlinear relationship (Figure 4). Depending on whether f_p and γ are related in the way predicted by the high or the low temperature limit, we can calculate an α using the appropriate model. It is important to emphasize that we expect each time-dependent measurement to give the same α over a range of γ, as long as the temperature remains constant.

2. The Para-H_2 Fraction

We are in the process of building a second DFG using a 532 nm cw-pump laser, a cw tunable dye laser, and an MgO-doped $LiNbO_3$ nonlinear crystal which will be capable of generating light in the range of 2.1-4.8 μm. Employing this new system with cavity ringdown in the hollow cathode, we can measure the rovibrational *para*-H_2 $S(0)$ transition at 4497 cm^{-1} and the S(1) *ortho*-H_2 transition at 4713 cm^{-1}. The ability to observe the *para*-H_2 S(0) and the *ortho*-H_2 S(1) transitions will enable us to investigate another aspect of the $H_3^+ + H_2$ reaction, namely, what is happening to the *para*-H_2 fraction (γ). The experiments of [28] used an exponential decay to model the decrease in the *para*-H_2 fraction. Our new DFG will give us the ability to measure this fraction *in situ*.

Throughout our analysis of this problem, we have assumed that this fraction remains constant due to the high number density of H_2 in comparison to H_3^+. If instead we allow the fraction to vary ($d\gamma/dt \neq 0$), we calculate values for γ over time that are very different from the starting value. Figure 5 shows γ versus time for different temperatures. The low temperature model predicts that the time constant for γ decay will change at different temperatures, whereas there is no such dependence in the high temperature model.

We will observe the decay of γ at the two temperatures in the hollow cathode, where the

$H_3^+ + H_2$ reaction is the dominant mechanism affecting the H_2 spin populations. Both the S(0) and S(1) transitions are observable at low temperature, but the *ortho*-H_2 transition S(1) is too weak to measure at the higher temperature, even with ringdown spectroscopy. We will determine γ at the higher temperature using the S(0) transition and the known number density of H_2 gas in the hollow cathode. In addition, we will monitor the equilibrium value ($\sim$ 10 ms) of γ when using normal 3:1 hydrogen. If the low temperature model is correct, then we should observe an equilibrium *para*-H_2 fraction that is higher at low temperature than the expected 25% for normal hydrogen. These measurements will provide additional evidence either for or against the low temperature model.

As stated earlier, the γ in dense clouds is enriched in comparison to the fraction expected for normal H_2 at the temperatures of formation [10, 11]. Figure 5 shows that the calculated equilibrium value of γ is greater than 90% *para*-H_2 at the the temperatures of dense clouds ($\sim$ 30 K), indicating that the $H_3^+ + H_2$ reaction may be the major driver of this enrichment. Not only is it important to understand the mechanism by which the *para*-H_2 fraction is changing, but this knowledge will translate to better dense cloud models which are essential to understanding astrochemical processes (e.g. formation of H_2D^+) [35] in regions where direct observation is not possible.

3. Supersonic Expansion Measurements

We intend to use cavity ringdown spectroscopy to measure the fraction of *para*-H_3^+ (f_p) in a supersonically expanding plasma over a wide range of *para*-H_2 feed gas enrichments (γ). As with the hollow cathode experiments, this will allow us to characterize the relationship between f_p and γ (Figure 3), but at even lower temperatures. We will use either the newly developed DR pulsed piezo source or a continuous source that is currently being tested for the SCRIBES ion beam experiment in our group [36]. These expansion experiments will also serve to verify our earlier measurement of $\alpha = 0.78$, or update this value if our findings indicate that the non-linear low temperature approximation is more accurate.

By sampling f_p and γ in different regions of the expansion, we can obtain measurements for α at a range of temperatures below 100 K. As with the low temperature hollow cathode experiments, we do not know which model we will use to calculate α, but this will become apparent once the experiment is complete.

IV. CONCLUSIONS

H_3^+ and H_2 play an important role in the chemistry of the interstellar medium. The different spin modifications of these species provide a useful astrophysical probe. Understanding how the conditions of the interstellar medium affect the spin modification budget of H_3^+ and H_2 is therefore essential.

We have found that the dissociative recombination rates of *ortho*- and *para*-H_3^+ differ by a factor of 2, but we will continue this study in the interest of obtaining a more precise, useful rate coefficient and to observe the dissociative recombination of H_3^+ enriched in a single quantum state.

We have also measured a value for $\alpha = k_{\mathrm{Hop}}/k_{\mathrm{Exchange}} = 0.78$ that seems to explain the observed fraction of *para*-H_3^+ in diffuse clouds. Unfortunately, our understanding is limited because we are not certain if this value truly represents a change in these reaction rates, or a change in available *ortho*- and *para*-H_3^+ states. Our studies will continue by using a hollow cathode and a supersonic expansion to gain a better understanding of this, and to obtain values of α at a wider range of temperatures. Measurements of S(0) and S(1) in the hollow cathode will help us understand how the spin states of H_2 are affected. This knowledge will provide a more solid foundation upon which we can build our models of hydrogenic species in the interstellar medium, knowledge that will allow us to use these important molecules as a probe to understand distant astrophysical processes and conditions.

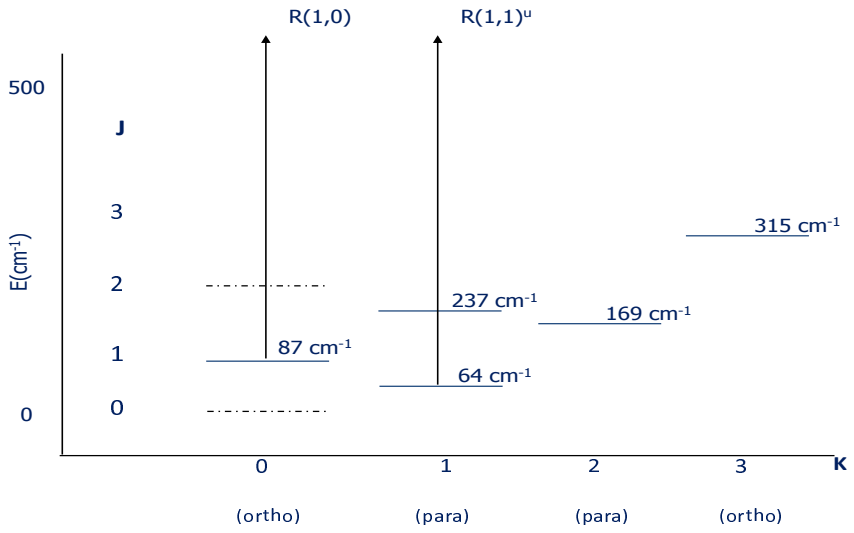

FIG. 1: Ground and low lying states of H_3^+. The primary transitions used in this experiment are depicted.

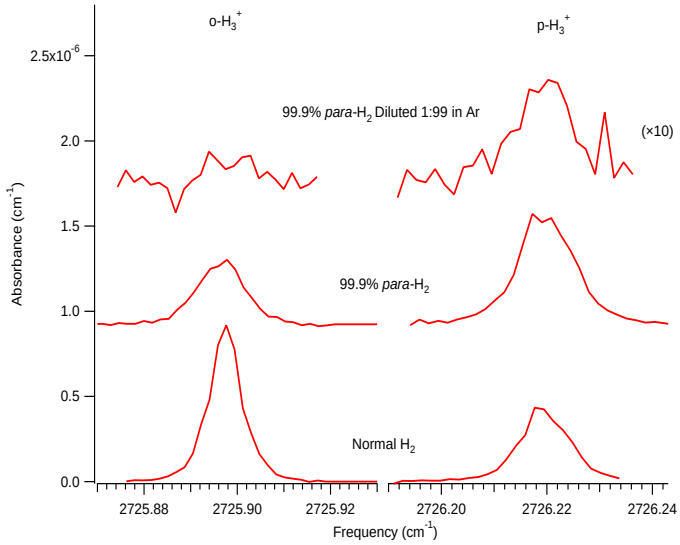

FIG. 2: Comparison of spectra for H_3^+ for various precursor gas purities. The plots are shifted vertically for clarity.

TABLE I: The percent of H_3^+ observed in the discharge when using pure and argon-diluted gases of varying initial *para*-H_2 enrichment.

% *para*-H_2 enrichment (γ)	% H_2 in Argon[a]	% *para*-H_3^+ (f_p)[b]
50	100	49.5 ± 0.4
97	100	73.9 ± 1.2
	1	82.8 ± 1.3
99.9	100	77.6 ± 1.6
	0.8	84.5 ± 1.1

[a]The percent dilution was calculated using pressure (P_{para-H_2}/P_{total})

[b]The reported errors are 1σ.

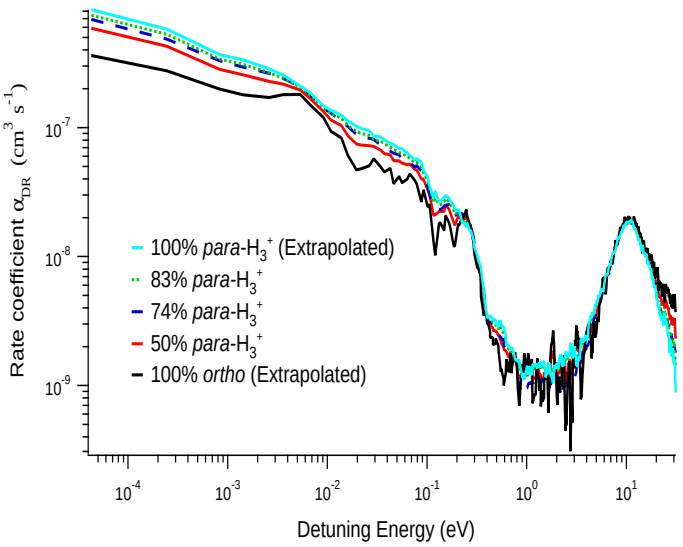

FIG. 3: Comparison of the H_3^+ dissociative recombination rate spectra for various enrichments of *para*-H_3^+. Calculated spectra for 100% *ortho*- and *para*-H_3^+ are also shown.

TABLE II: The branching ratios for spin conversion in the reaction $H_3^+ + H_2 \rightarrow H_3^+ + H_2$. The labeling (x,y) indicates the nuclear spins (I) of the various hydrogen species. For example (3/2,0) symbolizes (*ortho*-H_3^+, *para*-H_2).[a]

Reactant Spin Species	Weight	Type	(3/2,1)[b]	(3/2,0)	(1/2,1)	(1/2,0)
(3/2,1)	12	Identity	6/5	0	0	0
		Hop	12/5	0	6/5	0
		Exchange	19/5	1	8/5	4/5
(3/2,0)	4	Identity	0	2/5	0	0
		Hop	0	0	6/5	0
		Exchange	1	3/5	4/5	0
(1/2,1)	12	Identity	0	0	6/5	0
		Hop	6/5	6/5	3/5	3/5
		Exchange	8/5	4/5	19/5	1
(1/2,0)	4	Identity	0	0	0	2/5
		Hop	0	0	3/5	3/5
		Exchange	4/5	0	1	3/5

[a]Results from Oka, ref. [21]

[b]The spin modifications of the products

TABLE III: The percent *para*-H_3^+ measured in the discharge is dependent on the enrichment of the *para*-H_2 gas used. α, as calculated from experimental results.

% *para*-H_2 $(\gamma)^a$	% *para*-H_3^+ $(f_p)^b$	$k_{\mathrm{Hop}}/k_{\mathrm{Exchange}}$ $(\alpha)^c$
99.9	77.6 ± 1.6	0.83±0.1
97.0	73.9 ± 1.2	0.66±0.06
90.0	74.4 ± 1.7	0.87±0.14
75	70.0 ± 14.2[d]	-
25.0	49.5 ± 0.4[d]	-
Average		0.78±0.14

[a]Starting *para*-enrichment of H_2.
[b]Percent *para*-H_3^+ at point of probe.
[c]Reported errors are one standard deviation.
[d]Value not used to calculate α.

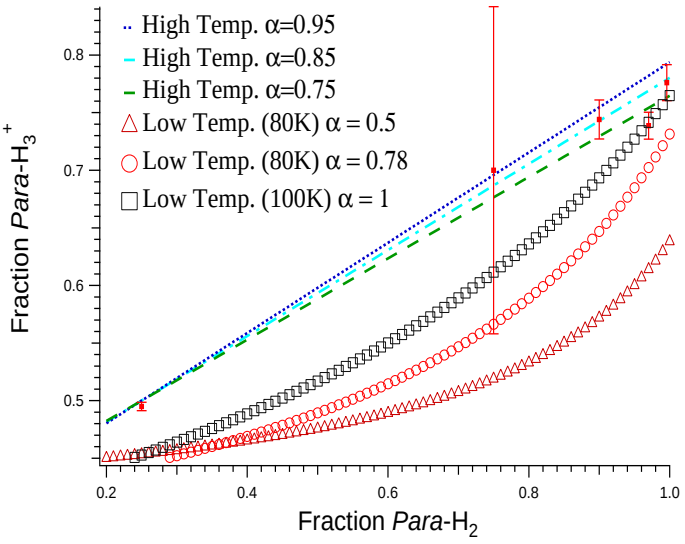

FIG. 4: Comparison of α, as calculated using the high temperature model (straight lines) and the low temperature model (curved lines). Experimental data are the points with error bars.

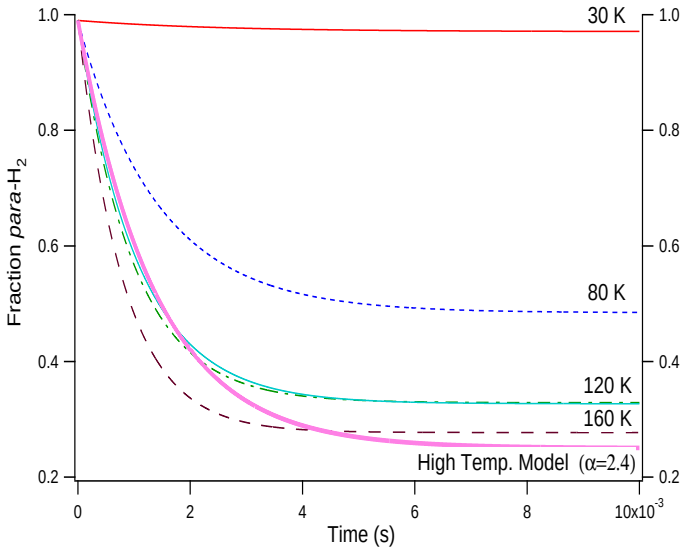

FIG. 5: The decay of the *para*-H_2 fraction (γ) with time according to the low temperature model. As the two 120 K lines (representing $\alpha = 0.78$ and 2.0) depict, the γ decay rate has a much stronger dependence on temperature than on $\alpha = k_{Hop}/k_{Exchange}$. According to the low temperature model, cold temperatures will result in a higher *para*-H_2 fraction, while the high temperature model (depicted by the solid pink line) predicts no temperature dependence.

[1] T. Oka, PNAS, **103**, 12235, (2006).

[2] N. Indriolo, T. R. Geballe, T. Oka, and B. J. McCall, Astrophys. J., **671**, 1736, (2007).

[3] T. R. Hogness, E. G. Lunn, Phys. Rev., **26**, 44, (1925).

[4] W. D. Watson, Astrophys. J., **183**, L17, (1973).

[5] E. Herbst and W. Klemperer, Astrophys. J., **185**, 505, (1973).

[6] W. Heisenberg. Z. f. Physik, **41**, 239, (1927).

[7] F. Hund, Z. f. Physik, **42**, 93, (1927).

[8] K. F. Bonhoeffer and P. Harteck, Naturwiss., **17**, 182, (1929).

[9] T. R. Geballe, B. J. McCall, K. H. Hinkle, and T. Oka, Astrophys. J., **510**, 251, (1999).

[10] J. .H. Lacy, R. Knacke, T. R. Geballe, and A. T. Tokunaga, Astrophys. J, **428**, L69, (1994).

[11] C. A. Kulesa, "Molecular Hydrogen and its Ions in Dark Interstellar Clouds and Star Forming Regions," Ph.D. Thesis, University of Arizona, (2002).

[12] B. J. McCall, A. J. Huneycutt, R. J. Saykally, N. Djuric, G. H. Dunn, J. Semaniak, O. Novotny, A. Al-Khalili, A. Ehlerding, F. Hellberg, S. Kalhori, A. Neau, R. D. Thomas, A. Paal, F. Österdahl, M. Larsson, Phys. Rev. A, **70**, 052716, (2004).

[13] H. Kreckel, M. Motsch, J. Mikosch, J. Glosík, R. Plašil, S. Altevogt, V. Andrianarijaona, H. Buhr, J. Hoffmann, L. Lammich, M. Lestinsky, I. Nevo, S. Novotny, D. A. Orlov, H. B. Pedersen, F. Sprenger, A. S. Terekhov, J. Toker, R. Wester, D. Gerlich, D. Schwalm, A. Wolf, and D. Zajfman, Phys. Rev. Lett., **95**, 263201, (2005).

[14] V. Kokoouline, C. H. Greene, Phys. Rev. A, **68**, 012703, (2003).

[15] S. F. dos Santos, V. Kokoouline, and C. H. Greene, J. Chem. Phys., **127**, 124309, (2007).

[16] B. A. Tom, Y. Miamoto, M. B. Wiczer, S. A. Bhasker, T. Momose, B. J. McCall,"*Ortho*- and *para*-H_2, Devices and Techniques for Converting and Quantifying the Enrichment of H_2 Nuclear Spin Modifications," in final preparation for Rev. Scientific Instr.

[17] A. Farkas, *Orthohydrogen, Parahydrogen, and Heavy Hydrogen*, Cambridge Univ. Press, (1935), p. 20-28.

[18] A. T. Stewart, and G. L. Squires, J. Scientific Inst., **32**, 26, (1955).

[19] R. Campargue, J. Phys. Chem., **88**, 4466, (1984).

[20] M. Quack, Mol. Phys., **34**, 477, (1977).

[21] T. Oka, J. Mol. Spec., **228**, 635, (2004).

[22] T. Oka, Molecular ions: Spectroscopy, Structure, and Chemistry, eds. T. A. Miller and V. E. Bondybay, North Holland-Amsterdam, (1983), p. 73.

[23] K. W. Busch and M. A. Busch, Cavity Ringdown Spectroscopy, eds. K. W. Busch and M. A. Busch, (1990), p. 7-19.

[24] C. M. Lindsday, and B. J. McCall, J. Mol. Spec., **210**, 60, (2001).

[25] H. Kreckel, A. Petrignani, M. Berg, D. Bing, S. Reinhardt, S. Altevogt, H. Buhr, M. Froese, J. Hoffmann, B. Jordan-Thaden, C. Krantz, M. Lestinsky, M. Mendes, O. Novotny, S. Novotny, H. B. Pedersen, D. A. Orlov, J. Mikosch, R. Wester, R. Plašil, J. Glosík, D. Schwalm, D. Zajfman, and A. Wolf, J. Phys.: Conf. Ser., **88**, 012064, (2007).

[26] B. A. Tom, R. D. Thomas, V. Zhaunerchyck, M. B. Wiczer, A. A. Mills, K. N. Crabtree, M. Kaminska, W. Geppert, M. Hamberg, E. Vigren, W. J. van der Zande, M. Larsson, B. J. McCall, "Dissociative recombination of highly enriched *para*-H_3^+," in final preparation for J. Chem. Phys.

[27] D. Gerlich, J. Chem. Soc. Faraday Trans., **89**, 2199, (1993).

[28] M. Cordonnier, D. Uy, R. M. Dickson, K. E. Kerr, Y. Zhang, and T. Oka, J. Chem. Phys., **113**, 3181, (2000).

[29] Y. Sheffer, M. Rogers, S. R. Federman, N. P. Abel, R. Gredel, D. L. Lambert, and G. Shaw, "Ultraviolet Survey of CO and H_2 in Diffuse Molecular Clouds: The Reflection of Two Photochemistry Regimes in Abundance Relationships," submitted and accepted to Astrophys. J., (2008).

[30] D. Proch and T. Trickl, Rev. Sci. Inst., **60**, 713, (1989).

[31] K. Park and J. C. Light, J. Chem. Phys., **126**, 044305, (2007).

[32] F. C. Van den Heuvel and A. Dymanus, Chem. Phys. Lett., **92**, 219, (1982).

[33] T. Amano, J. Chem. Phys., **92**, 11, (1990).

[34] J. U. White, J. Opt. Soc. Am., **32**, 285, (1942).

[35] D. Gerlich, E. Herbst, E. Roueff, Plan. Space Sci., **50**, 1275, (2002).

[36] A. Mills, Prospectus for Preliminary Examination, U. of Illinois, (2007).